Small Diameter Membrane Reflector Structures

M. Santer*

Imperial College London, London, SW7 2AZ, UK

K. Seffen† and A. Bonin‡

University of Cambridge, Cambridge, CB2 1PZ, UK

This paper proposes the use of membrane reflectors for space telescopes having apertures currently achievable using monolithic designs. It is shown, both analytically, and by numerical optimization, that membrane reflectors including necessary support structure may achieve comparable areal density to monolithic reflectors at a significantly reduced cost. Design formulae for the membrane reflector support structure are derived and validated.

I. Introduction

There is a current desire and need within the astronomical community to increase the resolution of space-based telescopes. This will enable the observation of small distant objects, for example extrasolar planets. Two of the major advantages of space-based compared to ground-based telescopes are that their view is not distorted by atmospheric effects, and that they may be designed to observe in the infrared portion of the spectrum.

Improved telescope resolution is achieved by increasing the diameter, or aperture, of the primary reflector. To make the launch of large aperture telescopes feasible it is necessary to decrease the weight required for a given aperture. The reduction of the areal density – the ratio of the structural mass to the telescope area – is one of the primary design drivers for new telescope concepts. For example the forthcoming James Webb Space Telescope (JWST) has an areal density, based on the total launch mass, that is 13 times smaller than the equivalently-calculated areal density for the Hubble Space Telescope (HST).[1]

As aperture size increases, it is necessary to consider how the telescope may be launched into space. The fairing volume of the launcher provides a design constraint. If the desired aperture is larger than the available space, it is necessary to design deployable structures that enable the telescope to be packed for launch and then deployed into their operating condition when in orbit.[2] The JWST for example will have a segmented primary reflector which is twice-folded for launch.[3] The design of deployable telescope mechanisms which provide sufficient positional accuracy is a complex and challenging task.

Membrane reflectors have been proposed as a technology which offers the potential to provide large apertures with very small areal densities. Many methods have been proposed for the deployment of large aperture membrane reflectors including, for example, the use of inflatable boundary supports.[4] One of the major barriers to their use, however, is that there is a large of heritage technology on which to base large aperture missions. The large inherent risk in considering such an untried technology for a large aperture mission is a strong disincentive to their use. In addition, interferometry techniques may be used to obtain large-aperture resolutions from constellations of small telescopes using current monolithic reflector technologies.[5] Although improvements in precision formation flying are necessary, the use of heritage reflector technology means that the perceived risk is lower. The planned DARWIN mission, for example, will use such an interferometry-based approach.[6]

The solution proposed in this paper to the problem of lack of heritage of membrane reflectors is to recognise that, while the possibility of extremely large apertures is attractive, it is worthwhile to focus

*Lecturer in Aerostructures, Department of Aeronautics, Prince Consort Road, London SW7 2AZ, Member AIAA. Email: m.santer@imperial.ac.uk

†Senior Lecturer, Department of Engineering, Trumpington Street, Cambridge CB2 1PZ, Member AIAA.

‡Research Student, Department of Engineering, Trumpington Street, Cambridge CB2 1PZ, Student Member AIAA.

initially on small apertures comparable to what may be achieved currently using monolithic technologies. This means that it is not necessary to consider sources of complexity, such as the incorporation of deployment. The main advantage of focussing on small membrane reflectors is that they are highly competitive on cost grounds. This is due both to the lower material cost, but also to the fact that they do not require the high-precision grinding and polishing that is required for monolithic reflector surfaces.

Membrane reflectors could be used for small aperture space telescopes on the grounds that their low cost offsets the risk inherent in the use of a new technology. If such missions were successful, they could form the primary reflectors for interferometry missions for which large numbers of small reflectors are desirable. Most importantly, at this stage, heritage would have been provided for larger aperture missions for which the full potential of membrane reflectors would be realized.

Following this introduction, this paper considers the minimum structural requirements for a simple membrane reflector concept and illustrates that they provide competitive performance at small diameters. The chosen concept is first introduced and a reference design is chosen for illustrative purposes. An analytic solution for the achievable areal density of this reflector design is then derived which, in addition, indicates the key design metrics that must be considered. This analysis is then validated by means of a dual-objective finite element-based optimization approach. Finally, the results are discussed and conclusions are drawn.

II. Membrane Reflector Concept

In order to assess the potential for small-diameter membrane reflectors it is necessary to specify the required structural components in order to estimate the mass and hence the areal density. Polygonal membranes having n sides, $n > 6$, are envisaged which are discretely attached to the support structure at each vertex. Similar schemes have been proposed for solar sails.[7] Two membranes are offset from each other, one to provide the reflective surface, and one to act as an electrode. Curvature is applied to both membranes by means of an electrostatic pressure caused by the membranes being oppositely charged.[8,9]

The minimum required support structure consists of two polygonal rings to resist the forces imparted at the membrane vertices, and offset struts. These have two purposes: the first is to resist the loading caused by the electrostatic pressure; the second is to provide adequate spacing between the two membranes so they can assume the desired curvature. The polygonal rings and the two membranes prior to being subjected to electrostatic pressure are shown for a representative 8-sided structure on the left hand side of Fig. 1. The offset struts and the same membranes in their curved configuration are shown on the right hand side of the figure.

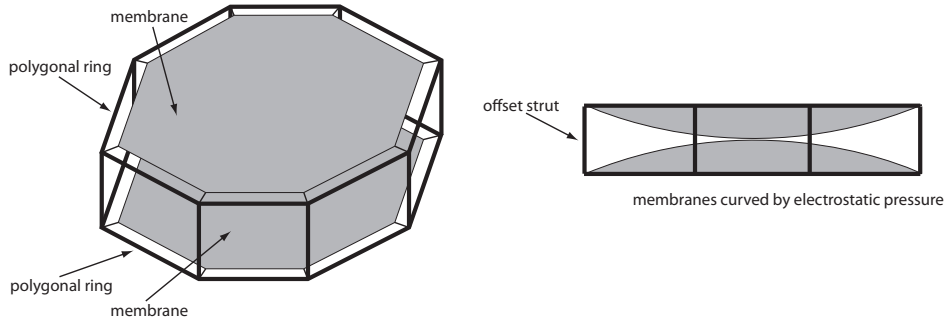

Figure 1. Membrane reflector including minimum required support structure concept

It must be emphasised that this is the minimum structure necessary to resist the loading imparted by the membranes. It is not intended to be a specific design – physical realizations may well require additional structure – but it is sufficient to be indicative of the likely achievable performance.

A. Reference Design

In addition to defining the reference geometry of the support structure, it is necessary to make material selections and to define the desired vibration and buckling performance, in order to estimate the performance. The actual choice is dependent on individual mission specifications, and the interaction with the remainder of

the telescope system. The values chosen below are intended to be characteristic of a broad range of potential missions.

The material chosen for the support structure is Silicon Carbide (SiC) which is used for the Herschel telescope's primary reflector structure.[10] It is an ideal material for space telescopes due to its high specific stiffness and high thermal stability. The Young's modulus is $E_s = 120$ GPa, and the density is $\rho_s = 3160$ kg/m^2. The membrane material is taken to be Mylar, with Young's modulus $E_s = 3.79$ GPa, Poisson's ratio 0.3, and thickness 14 μm. The applied pre-strain is $\epsilon_m = 15 \times 10^{-6}$.

It is necessary to define a representative central deflection of the membranes. This is, of course, mission specific, but an indicative value is 10% of the diameter i.e. $\delta = 0.1$ chosen. For reference, for the Herschel primary reflector, $\delta = 0.11$. A 10% margin against buckling, $\lambda = 1.1$ and a minimum resonant frequency $f_{min} = 45$ Hz is required. Again, the latter is the minimum specified resonant frequency of the Herschel telescope.

III. Analytical Solution

A. Support Structure Force Determination

In order to determine the forces on the support structure due to the prestrain and applied curvature of the membrane, we consider the regular n-sided polygonal membrane shown in Fig. 2a. The membrane has diameter, based on the circumscribed circle, of D, and the angle α, which describes each triangular segment of the polygon, is $2\pi/n$. The edge length a is therefore expressed as

$$a = D \sin\left(\frac{\alpha}{2}\right) \tag{1}$$

The vertices of the polygon are numbered sequentially counter-clockwise from 1 to n. Vertex 1 is always assumed to lie on the x-axis. The coordinates of the vertices are determined by

$$x_i = \left(\frac{D}{2}\right) \cos\left((i-1)\alpha\right), \; i = 1, ..., n \tag{2}$$

$$y_i = \left(\frac{D}{2}\right) \sin\left((i-1)\alpha\right), \; i = 1, ..., n \tag{3}$$

It is assumed that the polygonal membrane is connected to the support structure at each of its vertices and that the forces resulting from the prestrain and applied curvature are equally distributed and have value P. Vertical forces R, shown in Fig. 2b, are due only to the applied membrane curvature and are also assumed to be equally distributed between the vertices. We may express resultant forces in the positive x-direction and y-direction respectively as

$$P_x = P \sum_{i=1}^{n} \cos\left((i-1)\alpha\right)|_{x_i>0} = P\mathcal{C} \tag{4}$$

$$P_y = P \sum_{i=1}^{n} \sin\left((i-1)\alpha\right)|_{y_i>0} = P\mathcal{S} \tag{5}$$

in which $|_{x_i>0}$ indicates that the preceding function is only evaluated for $x_i > 0$. The geometric functions $\mathcal{C}$ and $\mathcal{S}$ are specified for convenience and compactness in the following analysis.

The support forces P consist of two components, one due to prestrain of the membrane, and one due to the applied curvature. These two components are denoted P_ϵ and P_κ and are determined separately and then superposed.

1. *Support Structure Force due to Membrane Prestrain*

It is assumed that prior to being deformed to the required curvature, the membrane is prestrained by an amount ϵ_m. This is necessary for two reasons: in real implementations, such a strain is useful to remove material wrinkles and to impart stiffness prior to out-of-plane deformation; in finite element analyses of the membrane, such as carried out in Sec. IV, the inclusion of prestrain provides geometric stiffness which aids convergence. If we consider material at the center of the membrane, in order to be able to neglect edge effects, we may express the assumed biaxial plane stress state as

$$\sigma_x \approx P_x/Dt \tag{6}$$

$$\sigma_y \approx P_y/Dt \tag{7}$$

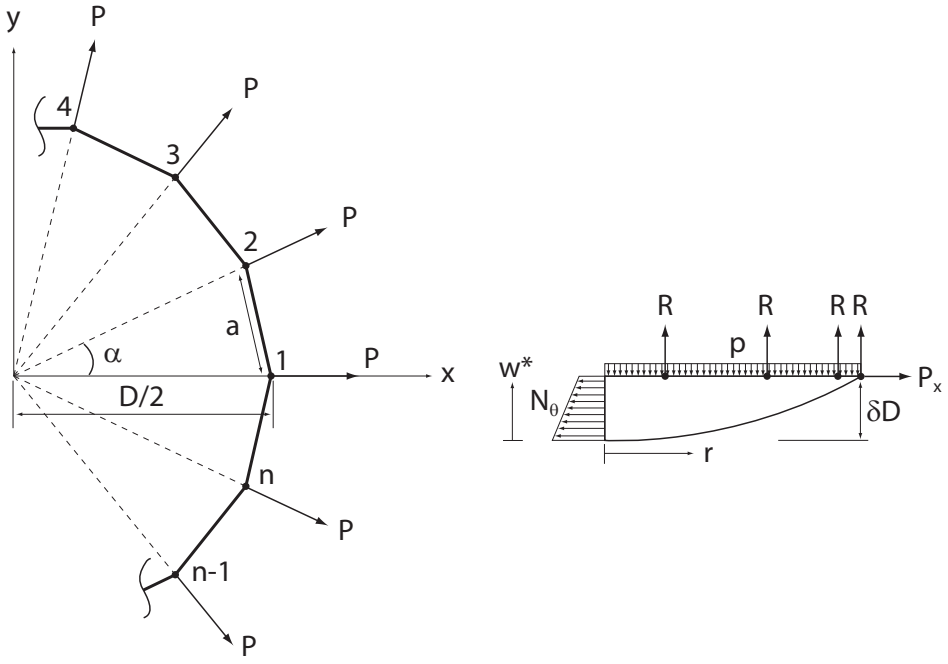

(a) (b)

Figure 2. Membrane parametrization and variable definition

in which t is the thickness of the membrane, and P_x and P_y are as defined in Eq. 4. These biaxial stresses may be represented by a single equivalent stress

$$\sigma_{eq} = \frac{1}{Dt}(P_x^2 + P_y^2 - P_x P_y)^{\frac{1}{2}} = \frac{P_\epsilon}{Dt}(\mathcal{C} + \mathcal{S} - \mathcal{CS})^{\frac{1}{2}} \tag{8}$$

This equivalent stress may then be related to the applied prestrain by means of Hooke's Law, allowing the applied force due to the prestrain at each vertex of the polygonal membrane P_ϵ to be written as

$$P_\epsilon = \frac{1}{(\mathcal{C} + \mathcal{S} - \mathcal{CS})^{\frac{1}{2}}} \frac{E_m \epsilon_m Dt}{(1 - \nu_m)} \tag{9}$$

in which E_m and ν_m are the Young's modulus and Poisson's ratio of the membrane material respectively.

2. Support Structure Force due to Membrane Curvature

In order to determine the support forces due to the membrane being deformed to the required curvature, further notation, shown in Fig. 2b, needs to be introduced. The center point of the membrane is required to deflect out-of-plane by an amount δD, for which δ is determined by particular mission requirements. This curvature is caused by a uniformly-applied pressure p, which is equilibrated by the forces R described above. To determine the forces P_κ, the membrane is cut along the y-axis which releases the membrane hoop-stresses N_θ. The distance up from the most highly-deformed central point is denoted by the variable w^*.

The free body diagram in Eq. 4 is used to determine the forces P_κ by evaluating moment equilibrium about the bottom left hand corner – the most highly-displaced point. This moment consists of the moment due to the hoop stress in the membrane M_σ, the moment due to the applied pressure M_p, the moment due to the vertical forces M_R, and the moment due to the forces P_κ denoted M_P. These are now evaluated in turn.

The hoop stress N_θ is evaluated by using Hencky's solution[11] for a circular membrane with a constant simply-supported boundary subject to uniform pressure loading, which is used to approximate the behaviour

of the polygonal membranes. This approximation is necessitated by the fact that no analytical solution for an n-sided polygonal membrane exists. Hencky's solution as been adopted for the analysis of circular membranes with continuously supported perimeters.[12] The error introduced by this approximation, which is to overestimate the structural stiffness, is reduced as n becomes larger, but must be acknowledged when interpreting the results. We define a dimensionless radius of the membrane

$$\hat{r} = \frac{r}{(D/2)} \tag{10}$$

Hencky's solution then gives

$$N_\theta = \frac{E_m t}{4} q^{\frac{2}{3}} \sum_0^\infty (2i+1) b_{2i} \hat{r}^{2i} \tag{11}$$

$$w^* = \delta D - \left(\frac{D}{2}\right) q^{\frac{1}{3}} \sum_0^\infty a_{2i} (1 - \hat{r}^{2i+2}) \tag{12}$$

in which the dimensionless pressure

$$q = \frac{pD}{2E_m t} \tag{13}$$

and the constants a_i and b_i depend on the membrane Poisson's ratio ν_m. For reference, values of a_i and b_i for $\nu_m = 0.2,\ 0.3,\ 0.4$ are provided in Tab. 1. The moment due to membrane hoop stress about the deflected central point of the membrane may now be expressed by the integral

$$M_\sigma = 2\left(\frac{D}{2}\right) \int_0^1 N_\theta w^* \mathrm{d}\hat{r} = \psi_1 p D^3 \tag{14}$$

in which the constant ψ_1 is determined using a Hencky series truncated to three terms. Values of ψ_1 are provided in Tab. 1. The moment due to the applied pressure is readily determined. For consistency, the

ν	a_0	a_2	a_4	b_0	b_2	b_4	ψ_1	ψ_2
0.2	0.5942	0.0623	0.0145	1.6827	-0.3531	-0.0494	0.0123	52.961
0.3	0.5799	0.0565	0.0123	1.7244	-0.3363	-0.0437	0.0131	58.612
0.4	0.5628	0.0502	0.0099	1.7769	-0.3167	-0.0376	0.0139	66.201

Table 1. Membrane parameters for $\nu = 0.2, 0.3, 0.4$

membrane is once again approximated as circular. This moment may be shown to be

$$M_p = \frac{1}{12} p D^3 \tag{15}$$

If the force due to the applied pressure is equally distributed between the vertices, and once again consider a circular membrane to be representative of an n-sided polygonal membrane for consistency, we may write

$$R = \frac{p\pi D^2}{4n} \tag{16}$$

and hence the moment due to these reaction forces as

$$M_R = \sum_{i=1}^n R x_i|_{x_i>0} = \frac{\pi \mathcal{C}}{8n} p D^3 \tag{17}$$

Finally we may express the moment due to the support forces P_κ as

$$M_P = \delta D P_x = \delta D \mathcal{C} P_\kappa \tag{18}$$

By combining the moments in Eqs. 14, 15, 17, and 18, ensuring equilibrium, and rearranging, we reach the following expression for P_κ

$$P_\kappa = \left(\psi_1 - \frac{1}{12} + \frac{\pi \mathcal{C}}{8n}\right)\left(\frac{1}{\delta \mathcal{C}}\right) p D^2 \tag{19}$$

It only remains to determine an expression for the pressure required to achieve the desired central deflection. This is achieved by solving Eq. 12 equal to zero for $\hat{r} = 0$ which gives

$$p = \frac{\psi_2 \delta^3 E_m t}{D} \tag{20}$$

in which the constant ψ_2 is determined using a Hencky series truncated to three terms. Values of ψ_2 are provided in Tab. 1.

B. Support Structure Mass Estimates

In the previous section, expressions for the vertical reaction force R and the horizontal reaction force P (being the sum of P_ϵ and P_κ) , due to applied membrane prestrain and enforced curvature, were derived in Eqs. 16, 9, and 19 respectively. These solutions may now be used to determine analytical expressions for the minimum mass of the support structure required to achieve a desired stiffness. This stiffness is governed by both vibration and buckling requirements. These are expressed as a load factor λ, which is the margin of safety against buckling, and a minimum allowable frequency f_{min}.

1. Buckling-limited Mass Determination

Two potential buckling modes are considered. These are: buckling of an individual member of the polygonal ring component of the support structure under the action of force P; buckling of an individual member of the offset strut component of the support structure under the action of force R. The support structure is assumed to behave as a linear elastic material with Young's modulus E_s and density ρ_s. A section ABCD of the membrane support structure including the forces applied by the top and bottom membrane is shown in Fig. 3.

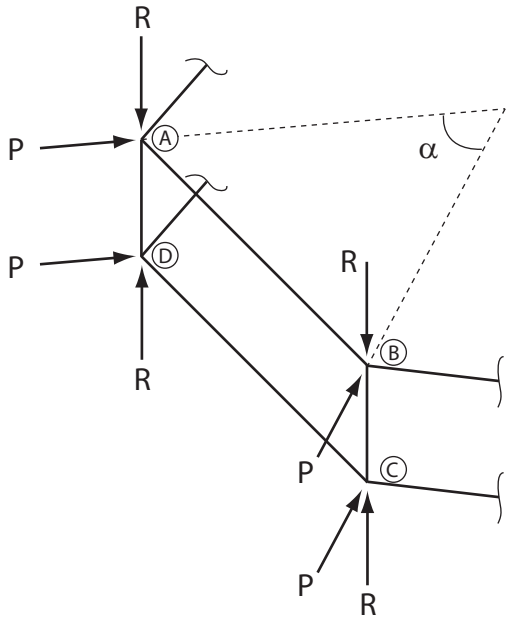

Figure 3. Support structure forces due to membrane prestrain and curvature on a single side consisting of two polygonal ring members and two offset struts

We first consider the buckling of the support structure under the action of forces P. It is sufficient to focus on a single member AB to determine the behaviour of the complete polygonal ring. Member AB will be subjected to axial loads at both ends equal to the component of P along the member. This means that we may express the required critical load of the member as

$$P_{crit} = \lambda P \sin\left(\frac{\alpha}{2}\right) \tag{21}$$

It is now necessary to consider the end restraint of member AB. At first glance it appears that both ends may best be approximated as built-in. It must be recalled, however, that when member AB buckles, the same critical load is present in all the other members forming the polygonal ring. If all the members have buckled, the ends of member AB, and similarly the ends of all the other ring members must rotate to maintain compatibility. For this reason, the critical load of member AB is determined assuming pinned ends to allow this rotation to occur.

If all the polygonal ring members are taken to have a circular cross-section with diameter d_{rb} for simplicity, It may be shown by equating Eq. 21 with Euler's well-known buckling formula that the required diameter to ensure adequate buckling resistance of the polygonal ring may be obtained from

$$d_{rb}^2 = 8D\sqrt{\frac{\lambda P \sin^3(\alpha/2)}{\pi^3 E_s}} \tag{22}$$

It is now possible to evaluate the volume and hence the mass m_{rb} of the polygonal ring structure to provide adequate resistance against buckling as

$$m_{rb} = 2\left(2\pi D\sqrt{\frac{\lambda P \sin^3(\alpha/2)}{\pi^3 E_s}}\right) nD\sin\left(\frac{\alpha}{2}\right)\rho_s \tag{23}$$

The required mass for the offset strut members of the support structure are determined in a similar way. In this case, the required critical load for each strut is λR, and the end fixation is determined to be both ends built-in on account of the restraint provided by the polygonal ring members. Again, we assume a circular cross-section for the offset struts for simplicity. The necessary strut diameter to ensure adequate resistance against buckling d_{sb} may be determined from

$$d_{sb}^2 = \sqrt{\frac{4\lambda\psi_2\delta^5 t D^3}{\pi^2 n}\left(\frac{E_m}{E_s}\right)} \tag{24}$$

and hence the mass m_{sb} of the offset struts to provide adequate resistance against buckling is

$$m_{sb} = \left(\frac{\pi}{4}\sqrt{\frac{4\lambda\psi_2\delta^5 t D^3}{\pi^2 n}\left(\frac{E_m}{E_s}\right)}\right) n(2\delta)D\rho_s \tag{25}$$

2. Frequency-limited Mass Determination

In order to determine the necessary support structural mass to achieve a design minimum frequency, it is necessary to consider the likely vibration modes of the structure. In a similar fashion to determining the required mass to resist buckling, the polygonal ring component and the offset strut component of the support structure are considered separately. We consider the polygonal ring first.

The polygonal ring is likely to resonate in one of two modes: an in-plane 'breathing' mode; and individual resonance of a single member such as member AB in Fig. 3. Which of these is the dominant resonant mode is determined by the geometry of a particular design. For this reason, the minimum mass calculation is based on both modes. The breathing mode for a 10-sided polygonal structure is shown in Fig. 4a. This mode corresponds to the polygon extending along one axis whilst simultaneously contracting along the other axis. An analytical solution for the resonant frequency of such a polygonal structure is not available. For this reason the structure is approximated as a circular ring, for which an analytical solution exists.[13] The breathing mode for a circular ring structure is shown in Fig. 4b. The circle is chosen to be the circle generated by the vertices of the undeformed polygon. This approximation is increasingly valid as the number of sides of the polygon n is increased.

Making this approximation, and assuming a circular member cross-section for simplicity, allows us to obtain the required diameter of the ring component of the support structure to provide a minimum breathing mode resonant frequency d_{rf1} from

$$d_{rf1}^2 = 5.485 f_{min}^2 D^4\left(\frac{\rho_s}{E_s}\right) \tag{26}$$

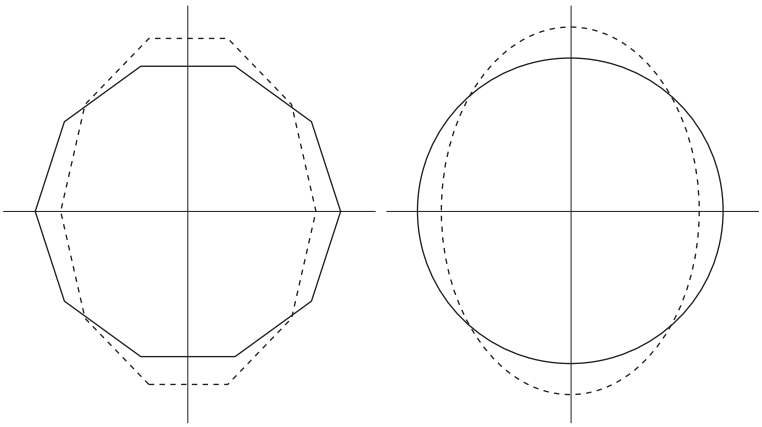

Figure 4. The breathing mode of a representative 10-sided polygonal support structure and the circular approximation to this structure

An analytical solution for the first resonant frequency if vibration of an individual member occurs exists[13] and allows us to obtain the required diameter of the ring component of the support structure to provide a minimum individual member vibration resonant frequency d_{rf2} from

$$d_{rf2}^2 = 28.169 f_{min}^2 D^4 \sin^4 \alpha \left(\frac{\rho_s}{E_s}\right) \tag{27}$$

The required ring member diameter to provide the required resonant frequency d_{rf} is therefore the maximum of Eqs. 26 and 27. The minimum required mass is therefore expressed as

$$m_{rf} = 2\left(7.042\pi f_{min}^2 D^4 \sin^4 \alpha \left(\frac{\rho_s}{E_s}\right)\right) nD \sin\left(\frac{\alpha}{2}\right)\rho_s \tag{28}$$

The calculation for the minimum required mass of the offset strut components of the membrane support structure is carried out in a similar fashion. The minimum diameter to ensure sufficient vibrational stiffness d_{sf} is obtained, as for Eq. 27, from

$$d_{sf}^2 = 28.169 f_{min}^2 (2\delta)^4 D^4 \left(\frac{\rho_s}{E_s}\right) \tag{29}$$

The minimum required mass of the offset struts is therefore

$$m_{sf} = \left(7.042\pi f_{min}^2 (2\delta)^4 D^4 \left(\frac{\rho_s}{E_s}\right)\right) n(2\delta) D\rho_s \tag{30}$$

It is now possible to estimate the minimum support structure mass m_{min} for any given design geometry and material selection, to provide a safety factor against buckling λ, and a minimum resonant frequency f_{min} from Eqs. 23, 25, 28, and 30 as

$$m_{min} = \sum (\max(m_{rb}, m_{sb}), \max(m_{rf}, m_{sf})) \tag{31}$$

The mass of the membrane is negligible in comparison to the mass of the support structure, and is therefore not included.

C. Key Design Metrics

The expressions determined in the previous section enable estimates for the achievable areal density of membrane reflectors to be determined. In the course of their derivation, however, additional relationships

are made clear. This are of particular use to determine which material properties and constraints are the predominant design drivers. Two metrics that are found to be crucial are the relative stiffness of the support and the membrane material (E_s/E_m), and the specific stiffness of the support structure (E_s/ρ_s). The best results in terms of areal density are achieved when these metrics are maximized. If the relative stiffness is increased, so too the buckling resistance. If the specific stiffness is increased, so too the first resonant frequency.

It is possible to to determine additional proportionalities inherent in the design. From Eq. 31 it may be seen that the frequency-limited mass is proportional to D^5 and f_{min}^2, and the buckling-limited mass is proportional to $D^{\frac{5}{2}}$ and $\lambda^{\frac{1}{2}}$. From this it may be inferred that for all except very small diameters, it is the minimum resonant frequency requirements that will drive the design of membrane reflectors.

D. Representative Design Performance

Having derived equations to determine the required structural mass for a membrane reflector, it is of interest to determine the performance for a representative design and to compare the results with existing monolithic reflector designs. The reference design that is considered is described in Sec. A.

The achievable areal density for polygonal membrane reflectors with a simple support structure consisting of two n-sided polygonal rings and n offset struts is evaluated using the required mass determined according to Eq. 31. This is divided by the effective aperture of a polygonal membrane, which is the circle which inscribes the polygon. Areal densities were evaluated for $n = 6,\ 8,\ 10,\ 12$, and $D = 0.5 - 3.5$ m and are plotted in Fig. 5. Areal densities – based on the monolithic primary reflector mass – for the 0.7 m Akari Telescope,[14] the 2.4 m Hubble Space Telescope, and the 3.5 m Herschel Telescope are also plotted.[10] These are 28 kg/m^2, 180 kg/m^2, and 22 kg/m^2 respectively, and are evaluated considering only the mass of the primary reflector to provide a legitimate comparison.

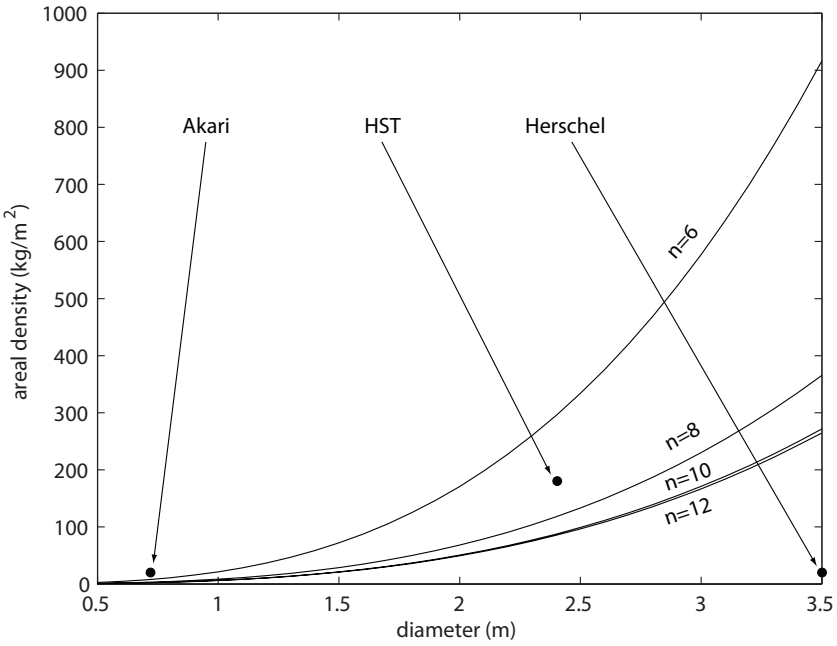

Figure 5. Achievable membrane reflector areal density prediction, for representative material properties and design parameters. Current monolithic reflector performances are included for comparison

It can be seen that the effect of increasing the number of sides of the polygonal membrane is to increase the achievable areal density. There is minimal improvement, however, above $n = 10$. It is also noted that the areal density that can be achieved by the simple membrane telescopes compares favorably to both Akari and HST. The proportionality of the areal density to D^3, however, means that the properties of the Herschel telescope may not be achieved without additional control. For this reason, it makes sense to focus preliminary

membrane reflector missions at smaller diameters. Below $D \approx 2.5$ m, membrane reflectors offer a simple cost-effective alternative to monolithic designs.

It must be emphasised that the areal densities plotted in Fig. 5 are not intended to be exact results, but are indicative of what may be achieved. There are sources of error in the analysis, in particular the assumption that the deflection of polygonal membranes may be modelled by circular membranes having the same diameter. In order to assess the validity of the analytical formulae derived above, and also to provide further insight into the behavior of the membrane reflectors, further work is needed . In the following section, optimal masses of structures having $D = 2.5$ m, which provide sufficient buckling and vibration resistance, are generated by coupling genetic optimization algorithms with nonlinear finite element analysis.

IV. Numerical Solution and Optimization

A. Optimization Strategy

For a given n-sided polygonal membrane of diameter 2.5 m, it is desired to determine the structure with minimal mass that provides a buckling factor $\lambda = 1.1$ and and minimum frequency $f_{min} = 45$ Hz. The out-of-plane deflection of the center of the membrane is required to be 10% of the diameter, i.e. $\delta = 0.1$. We do not know *a priori* what pressure is required to achieve the required central deflection. The design problem may therefore be specified as the dual-objective optimization

$$\begin{array}{ll} \min\,(\text{disp. error}) & \text{difference between actual and desired shape change} \\ \min\,(\text{mass}) & \text{mass of the support structure} \\ \text{s.t.} & \\ \lambda \geq 1.1 & \text{buckling constraint} \\ f_{min} \geq 45 \text{ Hz} & \text{frequency constraint} \end{array} \tag{32}$$

in which the design parameters are the applied membrane pressure, and the diameters of the polygonal ring d_r and offset struts d_s.

This problem could be solved in a single process, but it is computationally more efficient to subdivide it into two single objective optimization problems. The first optimization focusses on the membrane, which enables the required pressure and support structure loads to be determined. The second optimization applies the loadings determined in the first optimization to the support structure and evaluates the required member diameters.

The first optimization is expressed as

$$\begin{array}{ll} \min\,(\text{disp. error}) & \\ \text{s.t.} & \\ p < p_h & \text{pressure constraint} \\ f_{min} \geq 45 \text{ Hz} & \text{membrane frequency constraint} \end{array} \tag{33}$$

in which p_h is the required pressure determined analytically using Hencky's solution to achieve the desired central deflection of a circular membrane with equivalent diameter. The pressure constraint is to assist convergence of the problem – it is not a strict requirement of the analysis. It transpires that the frequency constraint is not active for the example diameter considered. The second optimization is then expressed as

$$\begin{array}{ll} \min\,(\text{support structure mass}) & \\ \text{s.t.} & \\ \lambda \geq 1.1 & \\ f_{min} \geq 45 \text{ Hz} & \text{support structure frequency constraint} \end{array} \tag{34}$$

for which the support structure is subjected to the applied loads determined in the first optimization. The variables are the diameter of the polygonal ring component of the support structure d_r, and the diameter of the offset strut components d_s. Both are permitted to vary continuously between 10 mm and 300 mm.

The primary advantage of decoupling the optimization problem in this way is that the solution of Eq. 33 requires computationally-expensive nonlinear analysis to determine the displacement of a membrane due to

an applied pressure. The optimization may be carried out with relatively few iterations, however, using a gradient-based algorithm. The solution of the optimization problem in Eq. 34 is not well suited to a gradient-based algorithm, as the determination of the buckling loads and resonant frequencies requires two eigenvalue analyses. A genetic algorithm requiring a large number of iterations is therefore preferred. This is not computationally expensive, however, as only linear analyses need to be carried out to determine the properties of the support structure.

The optimization algorithms are now described in greater detail. The gradient-based algorithm used is the Globally-Convergent Method. Sensitivities are based on a 0.01% perturbation of the variables, and the convergence tolerance is specified to be 0.01%. The genetic algorithm is based on binary coded individuals. A population consists of 20 individuals. Each individual generation has a 90% probability of single-point cross-over, and a 1% mutation probability. In addition, to ensue a sufficiently diverse population and to explore fully the design space, a rebirth strategy is used in which 50% of the population is replaced every 10 iterations. The fitness of individuals is assessed with a tournament selector method. As for the gradient-based algorithm, a convergence tolerance of 0.01% is specified.

1. Required Membrane Mesh Density

Before carrying out the optimization specified in Eq. 33 it is necessary to ensure that the membrane is modelled with sufficient accuracy whilst at the same time limiting the number of degrees of freedom to ensure that the optimization is as time-efficient as possible. In order to determine the best model configuration, an investigation was carried out based on a circular membrane – to enable comparison with Hencky's analytical solution – for various combinations of element type and mesh density. Only triangular membrane elements were considered with either zero or one mid-side node.

The finite element analysis first consists of the application of a biaxial prestrain $\epsilon_m = 15 \times 10^{-6}$ to impart geometric stiffness to the membrane. The applied pressure is then increased linearly up to the required value in a dynamic analysis. The Hilber-Hughes-Tayor solution method for the equations of motion is adopted with maximum damping factor $\alpha = 0.33$. The reason for the use of a dynamic analysis is that it provides unconditional stability and enables the solution to converge when the membrane has low curvature and low stiffness. When all the pressure is applied, the level is maintained and a single quasi-static analysis step is carried out to determine the final static configuration of the membrane.

Using this approach, the circular membrane mesh that gave the best results with fewest degrees of freedom was found to use second-order triangular elements with 30 elements around the membrane diameter. Consequently the same elements and a similar mesh density was used to analyse the polygonal membranes.

B. Optimal Support Structures

Using the optimization strategy described above, optimal support structure masses were determined for polygonal membranes with a diameter, as described by the vertices, of 2.5 m, and number of sides n = 6, 8, 10, 12, 14. In all cases considered, a converged solution to within 0.01% was obtained for both gradient-based and GA portions of the optimization. The achievable areal density and required number of optimization iterations are provided in Tab. 2. Areal densities evaluated using the analytical method derived in Sec. III are included in the table for comparison. The areal densities for both optimized and analytical solutions are plotted in Fig. 6.

	Iterations		Areal Density (kg/m^2)	
n	Grad.-based	GA	Optimized	Analytical
6	9	162	110	334
8	7	542	119	133
10	7	762	128	99
12	5	182	112	97
14	5	982	122	95

Table 2. Optimal areal densities and the required number of optimization iterations

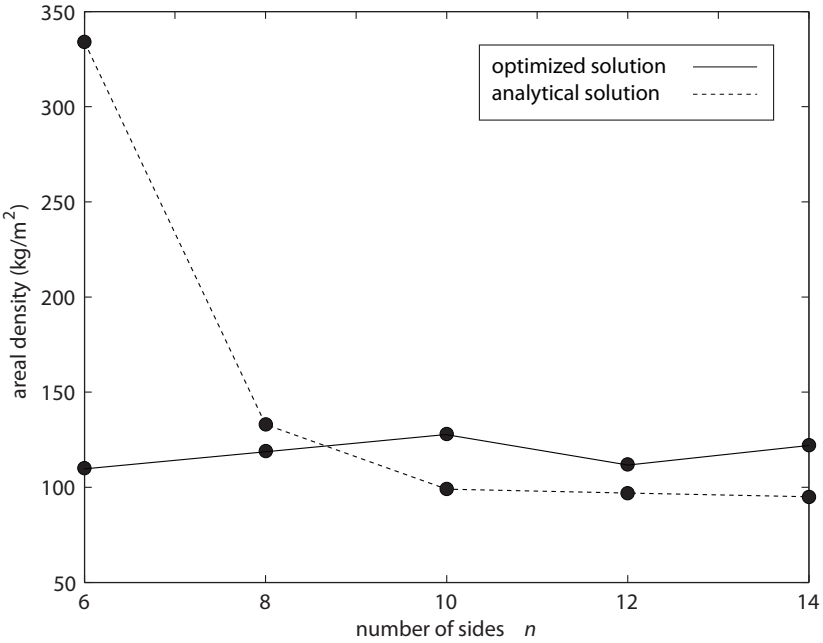

Figure 6. Areal density prediction, comparing optimal numerical and analytical solutions for 2.5 m diameter polygonal membranes

The pressure p, the diameters of the polygonal ring and offset struts d_r and d_s,and the required mass determined by the optimization are provided in Tab. 3 and are compared to the analytically determined values. The minimum frequency determined for the optimal solution is also provided for comparison in Tab. 4 – $f_{min} = 45$ Hz for all the analytical solutions.

n	p (Pa)	d_r (mm)	d_s (mm)	m (kg)	ω_{min} (Hz)
6	350	101	58	405	46.8
8	455	111	55	500	48.8
10	542	119	46	571	51.2
12	595	110	57	517	45.5
14	639	119	35	570	46.4

Table 3. Optimized applied pressure and support structure variables

V. Discussion

The results listed in Tab. 2 and plotted in Fig. 6 show that there is an excellent qualitative and reasonable quantitative relationship between the analytically-determined and optimized areal densities of the 2.5 m membrane reflector. The exception to this is for 6-sided membranes in which the analytical prediction is a substantial overestimate. The reason for this discrepancy is that Hencky's solution for the required membrane pressure is less valid for polygonal membranes with few vertices. The approximation is improved as the number of vertices n increases. It is noted that the support structure design for $D = 2.5$ m is controlled by the frequency requirements.

For $n \geq 8$, the derived analytical solution is a useful predictive tool for the achievable areal densities of membrane reflectors. It also provides valuable information concerning the relationships between the

n	p (Pa)	d_r (mm)	d_s (mm)	m (kg)
6	1244	182	9.7	1229
8	1244	121	9.7	558
10	1244	107	9.7	439
12	1244	107	9.7	441
14	1244	107	9.7	443

Table 4. Analytically determined applied pressure and support structure variables

variables and the key design drivers. It can be seen, however, from the results in Tables. 3 and 4, that the analytical expressions in their current form do not adequately predict the dimensions of the individual members of the offset strut components of the support structure. As mentioned above, the use of the pressure determined using Hencky's solution for a circular is an overestimate for polygonal membranes. In addition, the approximation of the offset struts as fully restrained at both ends for the frequency analysis, clearly results in them being too stiff. Quantitative predictions with the analytical expressions could be improved, if required, by the addition of correctional factors to reduce the pressure and the offset strut end fixity.

The most important results are observed in Fig. 5. It may be seen that membrane reflectors may achieve comparable areal densities to the HST and Akari Telescope. This uses a simple support structure, and has no requirement for active control to to the specification of a sufficiently high minimum frequency. This demonstrates that relatively cheap membrane reflectors can provide similar performance to monolithic designs for diameters less than 2.5 m and consequently are well worth consideration at this scale in order to provide heritage for large-aperture missions that could not be achieved using current technologies.

VI. Conclusions

This paper has derived analytical expressions which enable the achievable areal density of membrane reflectors to be predicted and compared to existing monolithic designs. These expressions were validated by comparison to optimized finite element results for a diameter of 2.5 m, and found to offer a reasonable prediction of areal density, particularly as the number of sides of the polygonal membrane is increased. If required, the expressions may be simply altered by the incorporation of additional factors to provide accurate predictions not only of the areal density, but also the support structure dimensions. A corollary of the derivation of the analytical expressions was the determination of metrics that govern the design, in particular that the dominant frequency-dependent mass is proportional to $D^{\frac{5}{2}}$.

The primary conclusion of this work is that it is worthwhile to develop relatively small diameter membrane reflector telescopes before focussing on very large aperture missions. Although small apertures may be achieved using monolithic reflector technology, they are more expensive that equivalent membrane-based designs. The most important outcome, however, would be the development of heritage technology for future large aperture missions.

In order to achieve membrane reflectors of any diameter, future work is required to ensure that an adequate optical surface may be achieved. In particular, this requires further understanding of the curvature that arises from electrostatic pressure and the degree of control this provides. Also membrane wrinkles at the discrete supports need to be predicted and eliminated. It has been seen that the structural performance of polygonal membrane reflectors is not a strong function of the number of sides. This therefore provides freedom to vary the number of sides to achieve the best possible reduction of wrinkling.

Acknowledgments

This work was carried out within the European Science Foundation Shape Control of Membrane Reflectors (SCMeRe) project in collaboration with the Université Libre de Bruxelles.

References

[1]Gardner, J., Mather, J., Clampin, M., Doyon, R., Greenhouse, M., Hammel, H., Hutchings, J., Jokobsen, P., Lilly, S., Long, K., Lunine, J., McCaughrean, M., Mountain, M., Nella, J., Reike, G., Reike, M., Rix, H., Smith, E., Sonneborn, G., Stiavelli, M., Stockman, H., Windhorst, R., and Wright, G., "The James Webb Space Telescope," *Space Science Reviews*, Vol. 123, 2006.

[2]Hedgepeth, J. and Adams, L., "Design concepts for large reflector antenna structures," NASA Contractor Report 3663, Contract NAS l-16134.

[3]Nella, J., Atkinson, C., Bronowicki, A., Bujanda, E., Cohen, A., Davies, D., Mohan, M., Pohner, J., Reynolds, P., Texter, S., Fitzgerald-Simmons, D., Waldie, D., Woods, R., Lynch, R., Lundquist, R., Menzel, M., Smith, B., Sullivan, P., Atcheson, P., and Lightsey, P., "James Webb Space Telescope (JWST) Observatory Architecture and Performance," *Proc. of the Space 2004 Conference and Exhibit*, Vol. AIAA Paper No. 2004-5986, 2004.

[4]Ruggiero, E., Bonnema, G., and Inman, D., "Application of siso and mimo Modal Analysis Techniques on a Membrane Mirror Satellite," *Proc. ASME Internation Mechanical Engineering Congress and Exposition*, 2003.

[5]Lay, O. and Blackwood, G., "Formation Flying Interferometry," *Proc. of the SPIE – Interferometry in Space*, Vol. 4852, 2003.

[6]ESA-SciA, "Darwin Mission Status Summary," Ref. SCI/AM/DARWIN-SUMSTAT/06, Issue 2, Revision 2, 2007.

[7]Sakamoto, H., Park, K., and Miyazaki, Y., "Evaluation of membrane structure designs using boundary web cables for uniform tensioning," *Acta Astronautica*, Vol. 60, pp. 846–857.

[8]Washabaugh, P. and Miller, R., "An effect of geometric scale on the configuration of large reflectors," *Aerospace Conference, 2003. Proceedings. 2003 IEEE*, Vol. 8, 2003, pp. 3995–4003.

[9]Angel, R., Burge, J., and Hege, K., "et al. Stretched Membrane with Electrostatic Curvature (SMEC): A New technology for Ultra-lightweight Space Telescopes," *Proc. SPIE, UV, Optical , and IR Space Telescopes and Instruments*, 2000.

[10]Sein, E., Toulemont, Y., Safa, F., Duran, M., Deny, P., de Chambure, D., Passvogel, T., and Pilbratt, G., "A Φ 3.5 m SiC telescope for HERSCHEL mission," *Proc. of the SPIE – IR Space Telescopes and Instruments*, Vol. 4850, 2003.

[11]Fichter, W., "Some solutions for the large deflections of uniformly loaded circular membranes," NASA Technical Paper 3658, URL: http://techreports.larc.nasa.gov/ltrs/ltrs.html.

[12]Jenkins, C., Kalanovic, V., Padmanabhan, K., and Faisal, S., "Intelligent shape control for precision membrane antennae and reflectors in space," *Smart Meter. Struct*, Vol. 8, pp. 857–867.

[13]Blevins, R., *Formulas for natural frequency and mode shape*, Van Nostrand Reinhold, New York, London, 1979, ISBN: 0442207107.

[14]Kaneda, H., Onaka, T., and Yamashiro, R., "Development of SiC Mirror for Astro-F," *Institute of Space and Astronautical Science Report*, , No. 14, 2000.